

INVESTIGATION OF RELATIVISTIC ELECTRON FLUXES ON INTERNATIONAL SPACE STATION BY R3DR INSTRUMENT

Tsvetan Dachev¹, Borislav Tomov¹, Yury Matviichuk¹, Plamen Dimitrov¹,
Nikolai Bankov¹, Guenther Reitz², Gerda Horneck², Donat-Peter Häder³, Michael Lebert⁴,
Martin Schuster⁴

¹Space Research and Technology Institute – Bulgarian Academy of Sciences

²DLR, Institute of Aerospace Medicine, Köln, Germany

³Neue Str. 9, 91096 Möhrendorf, Germany

⁴Department für Biologie der Friedrich-Alexander-Universität, Ökophysiologie der Pflanzen Erlangen, Germany
e-mail: tdachev@bas.bg; Guenther.Reitz@dlr.de; gerda.horneck@dlr.de; donat@dphaeder.de;
mlebert@biologie.uni-erlangen.de; mschuste@biologie.uni-erlangen.de

Keywords: Space radiation, Space weather, Dosimetry, Spectrometry

Abstract: The paper presents observations of relativistic electron precipitations (REP) on the International Space Station (ISS) obtained by Bulgarian build R3DR instrument in the period March 2009-August 2010. R3DR is a Liulin type spectrometer-dosimeter with a single Si PIN detector 2 cm² of area and 0.3 mm thick. The total external and internal shielding before the detector of R3DR device is 0.41 g cm⁻². The calculated stopping energy of normally incident particles to the detector is 0.78 MeV for electrons and 15.8 MeV for protons. Electrons with energy higher than 0.78 MeV play important role for the formation of the space radiation doses of the astronauts during Extra Vehicular Activity (EVA). The global distribution of the REP generated fluxes and absorbed doses at the orbit of ISS are analyzed. The REP in April 2010 being the second largest in GOES history >2 MeV electron fluence event is specially studied and compared with models and data from other satellites.

ИЗСЛЕДВАНЕ НА ПОТОЦИТЕ ОТ РЕЛАТИВИСТИЧНИ ЕЛЕКТРОНИ НА МЕЖДУНАРОДНАТА КОСМИЧЕСКА СТАНЦИЯ С ПРИБОРА R3DR

Цветан Дачев¹, Борислав Томов¹, Юрий Матвийчук¹, Пламен Димитров¹, Николай Банков,
Гюнтер Райтц², Герда Хорнек², Донат-Петер Хедър³, Михаел Леберт⁴, Мартин Шустер⁴

¹Институт за космически изследвания и технологии – Българска академия на науките

²DLR, Institute of Aerospace Medicine, Köln, Germany

³Neue Str. 9, 91096 Möhrendorf, Germany

⁴Department für Biologie der Friedrich-Alexander-Universität, Ökophysiologie der Pflanzen Erlangen, Germany
e-mail: tdachev@bas.bg; Guenther.Reitz@dlr.de; gerda.horneck@dlr.de; donat@dphaeder.de;
mlebert@biologie.uni-erlangen.de; mschuste@biologie.uni-erlangen.de

Ключови думи: Космическа радиация, Космическо време, Дозиметрия, Спектрометрия

Абстракт: Представени са резултатите от наблюденията на изсипвания на релативистични електрони (ИРЕ) на Международната космическа станция (МКС), получени със създадения в България прибор R3DR в периода март 2009-август 2010 г. R3DR е спектрометър-дозиметър от типа „Люлин“ с единичен силициев Si PIN детектор с площ от 2 cm² и дебелина от 0.3 mm. Тоталната вътрешна и външна защита на детектора е 0.41 g cm⁻². Изчислената енергия на спиране на електроните е 0.78 MeV, а на протоните е 15.8 MeV. Електроните с енергия по-голяма от 0.75 MeV играят важна роля за формирането на дозата от космическа радиация на космонавтите по време на дейност извън космическия кораб. Анализирани са глобалното разпределение на генерираните по време на ИРЕ потоци и абсорбирани дози на МКС. Експерименталните ИРЕ данни за м. април 2010 г., които са вторите по големина на флуенса от електрони с енергия повече от 2 MeV в историята на наблюденията на спътниците от серията GOES, са изследвани подробно и са сравнени с данни от теоретични модели и други спътници.

1. Introduction

Relativistic electron precipitations (REP) have been observed for many years. First reports are by (Brown and Stone, 1986) and (Imhof et al. 1986, 1991). The most comprehensive study of long-term observations of REP was made by Zheng et al. (2006), using the 2–6 MeV electron data from the SAMPEX satellite during 1992–2004.

Relativistic electrons enhancements in the outer radiation belt are one of the major manifestations of space weather (Zheng et al., 2006; Wrenn, 2009) near the Earth's orbit. Their understanding is of significant importance from both a practical and space radiation physics point of view. Electrons with energies of a few MeV can penetrate the spacecraft shielding and can deposit significant charge in the dielectric materials, which after electrostatic breakdown can damage sensitive electronic preamplifiers and whole systems of the spacecraft. A similar event happened with the Galaxy 15 spacecraft (Green et al., 2010), which stopped responding to ground commands at the beginning of the period studied by us on 5th of April at 09:48 UTC.

Relativistic electrons were observed by us outside the Foton M2/M3 spacecraft in the periods 31 May–16 June 2005 and 14–29 September 2007 and outside the European Columbus module of the ISS in 2008 (Dachev et al., 2009). The relativistic electrons observed on ISS in 2008 were connected with the geomagnetic field disturbances in the period 27/02/2008-07/05/2008.

Now we present the full range of data obtained by R3DR instrument in the period between January and August 2010. The main idea of the analysis of more than 150 daily fluences is to underline that the REP events are common on ISS. Never the less that the obtained doses do not pose extreme risks for the astronauts being on EVA they have to be considered as permanently observed source, which require additional comprehensive investigations.

2. Instrument description

The R3DR instrument is a successor of the Liulin-E094 instrument, which was part of the experiment Dosimetric Mapping-E094 headed by Dr. G. Reitz that was placed in the US Laboratory Module of the ISS as a part of Human Research Facility of Expedition Two Mission 5A.1 in May-August, 2001 (Reitz et al., 2005, Dachev et al., 2006, Wilson et al., 2007, Nealy et al., 2007, Slaba et al., 2011).

The experiments with the R3DR spectrometer were performed after successful participations in ESA Announcements of Opportunities, led by German colleagues Dr. Gerda Horneck and Prof. Donat-P. Häder (Horneck et al., 1998). The spectrometers were mutually developed with the colleagues from the University of Erlangen, Germany (Streb et al., 2002, Häder et al., 2009).

The R3DR spectrometer was launched inside the EXPOSE-R facility (Please see Figure 1) at the outside platform of Russian Zvezda module at the ISS in December 2008. The first data were received on March 11, 2009. Till 27th of January 2011 the instrument was working almost permanently with 10 seconds resolution in a very similar way as the R3DE instrument on the Columbus module (Dachev, 2009). R3DR instrument is a low mass, small-dimensioned automatic device that measures solar radiation in 4 channels and ionizing radiation in 256 channels. It is Liulin type energy deposition spectrometer. The size of the aluminum box of the R3DR instrument is 76 x 76 x 34 mm.

The ionizing radiation is monitored using a semiconductor PIN diode detector (2 cm² in area, 0.3 mm thick). Its signal is digitized by a 12 bit fast A/D converter after passing a charge-sensitive preamplifier. The deposited energies (doses) are determined by a pulse height analysis technique and then passed to a discriminator.

The amplitudes of the pulses $A[V]$ are transformed into digital signals, which are sorted into 256 channels by a multi-channel analyzer. At every exposition time interval one energy deposition spectrum is collected. The energy channel number 256 accumulates all pulses with amplitudes higher than the maximal level of the spectrometer of 20.83 MeV. The methods for characterization of the type of incoming space radiation are described by (Dachev, 2009).

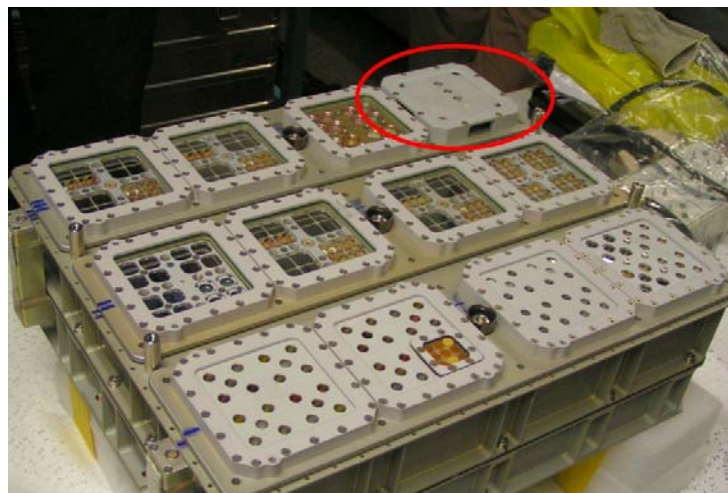


Figure 1. External view of the EXPOSE-R facility. The R3DR instrument is situated inside the red oval.

System international (SI) determination of the dose is used, in order to calculate the detector doses absorbed in the silicon. SI determines that the dose is the energy in Joules deposited in one kilogram. The following equation is used:

$$D[Gy] = K \sum_{i=1}^{256} (EL_i i)[J] / MD[kg] \quad (1)$$

where K is a coefficient, MD - the mass of the solid state detector in [kg] and EL_i is the energy loss in Joules in channel i . The energy in MeV is proportional to the amplitude A of the pulse $EL_i[MeV] = A[V] / 0.24[V/MeV]$. $0.24[V/MeV]$ is a coefficient depending on the used preamplifier and sensitivity of it used.

The construction of the R3DR box consists of 1.0 mm thick aluminum shielding before the detector. The total shielding of the detector is formed by additional internal constructive shielding of 0.1 mm copper and 0.2 mm plastic material. The total external and internal shielding before the detector of R3DR device is 0.41 g cm^{-2} , respectively. The calculated stopping energy of normally incident particles to the detector is 0.78 MeV for electrons and 15.8 MeV for protons (Berger et al., 2010). This means that only protons and electrons with energies higher than the above mentioned could reach the detector.

3. R3DR data analysis

The available R3DR data covered 2 main periods: March-June 2009 and December 2009-August 2010. Except the large data gap between July and January 2009 there are two smaller periods in January-February 2010 and in the middle of March 2010.

The selection procedure, which allows us to distinguish between 3 different radiation sources (GCR, SAA and ORB) seen by the R3DE instrument, is based on the analysis of the dose to fluxes values (Dachev, 2009) and on the methodology described in Bankov et al. (2010).

Figure 3 accumulates in the bottom panel all available R3DR relativistic electrons daily fluences (ISS Flu) and daily absorbed dose rates (ISS AD) data. These measurements were compared with the GOES-11 daily fluence data for energies above 2 MeV and the daily global Ap index (upper panel). All curves represent the moving average over 2 points of the raw data.

The most interesting period in Figure 4 began on 1st of April 2010 and covered all data till 20th of August. The R3DR and GOES-11 daily relativistic electron fluences almost explosively increased on 6th and 7th of April as seen on Figs. 4 and 5. The consequences of the space weather processes, which provoked this increase can be described as follows (Space Weather Highlights, 05-11 April 2010, SWO PRF 1806, 13 April 2010, (<http://www.swpc.noaa.gov/>): 1) Solar activity was at very low levels with isolated low-level B-class flares; 2) a halo coronal mass ejection (CME) is observed on 03/0954 UTC; 3) About 2 days later a shock was observed at ACE at 05/0756 UTC, which led to a sudden impulse on Earth at 05/0826 UTC (38 nT was observed at the Boulder magnetometer); 4) the ACE satellite observed wind speeds between $720\text{-}800 \text{ km s}^{-1}$ behind the shock, with B_z reaching values around -15 nT ; 5) the activity continued on 06 April with predominantly active to minor storm levels, as well as an interval of minor to major storm levels

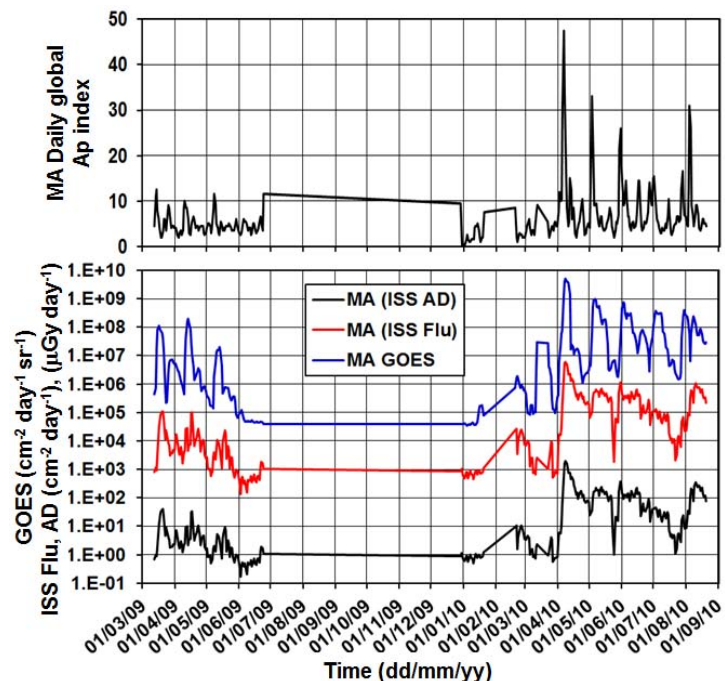


Fig. 2. Results for the daily $>0.78 \text{ MeV}$ fluence measured with the R3DE instrument on ISS (ISS flu???) and the dose rate (ISS AD) deposited by it for the whole operational time between February 2008 and September 2009. These data are compared with the daily GOES-11 satellite $>2 \text{ MeV}$ (GOES) fluence and the daily global Ap index.

observed between 06/0000-0600 UTC; 6) Wind speeds at ACE decreased to about 550 km/s at 06/2100 UTC.

Nevertheless that the created magnetic storm on 6th of April was moderate (daily $A_p=49$, minimal $Dst=-72$ nT at about noon), the second largest in history of GOES fluences of electrons with energies >2 MeV were measured. The increase in the GOES-11 fluence of electrons with energies

more than 2 MeV was by 4.5 orders of magnitude, while the $R3DR > 0.78$ MeV fluences increased less than 4 orders of magnitude. Till the end of measurements with the R3DR instrument at 20th of August 2010, a few smaller A_p maxima were observed and they were followed by very similar responses on the GOES satellite, while the ISS data correlation was much smaller.

Fig. 3 aims to present the geographic distribution of the data for the period 1st of April-7th of May 2010. Geographic longitude and latitude are on the X and Y axes, respectively. The white (white blue) curves represent equal McIlwain's - L-parameter values (McIlwain, 1961; Heynderickx et al., 1996) at the altitude of the station. The closed line in the eastern Hemisphere represents $L=1$. Other open lines rise with values 1.5, 2.5, 3.5 and 4.5 from the equator toward the poles. The dose rate is in the 3rd dimension and the values are colour coded by the logarithmic scale bar shown at the right side of the graphic. The dose rate values presented are obtained by averaging of the rough data in longitude/latitude squares with 1° size. The regions ORB and SAA regions are labelled.

The SAA region is well seen in Fig. 3. The coordinates of its central location are remarkable, which are at -50° west longitude and -32° south latitude for the dose rate. The flux maximum location is at the same longitude but at -30° south latitude. These values are in comparison with AP-8 MIN model (SPENVIS (<http://www.spennis.oma.be/>); (Vette, 1991) epoch 1970 moved with -12° to the west and the flux maximum with 2° moved to the north (Wilson et al. 2007). The calculated rate of the flux maximum movement is $0.3^\circ \text{ yr}^{-1}$ to the west and $0.05^\circ \text{ yr}^{-1}$ to the north. These drift rate values are in good agreement with (Badwar et al., 1994) and with (Fürst et al., 2009), but slightly disagree with our previous findings (Wilson et al. 2007) of $0.19^\circ \text{ yr}^{-1}$ westward drift.

The Relativistic electron precipitations (REP) regions are parts of the outer radiation belts (ORB) and are seen in both Hemispheres as bands of high dose rate values in the range $3.5 < L < 4.5$. The Northern Hemisphere REP dose rate values have a single area situated between 50°W and 130°W with a maximum at 90°W . In the Southern Hemisphere the REP is a wide area between 20°E and 170°W . A well-defined maximum is formed at about 70°E . Further high values dose rates are randomly distributed in the whole area up to 180°E . The Northern Hemisphere REP maximum lies above 45°N rising toward the maximum inclination of ISS at 51.8° . In the Southern Hemisphere the maximum is wider, starting from 42°S . There is a well seen maximum at about 48°S . The presentation of REP data in the L value coordinates shows a maximum at about $L=3.9$ in both Hemispheres. Due to the Earth magnetic field asymmetries the maximal L value in Northern Hemisphere is $L=4.64$, while for the Southern Hemisphere the maximal value is $L=6.14$. This asymmetry is probably the reason for the maximal dose rate values in the Northern Hemisphere to be about $6000 \mu\text{Gy h}^{-1}$, while the Southern Hemisphere maximal dose rate values are more than 3 times larger and reach $22,000 \mu\text{Gy h}^{-1}$.

The GCR dose rate values are also well seen in Figure 4 as enhanced bands with values between 0.5 and $10 \mu\text{Gy h}^{-1}$ equatorwards from the REP bands.

The averaged L value distributions of the dose rates of the three major radiation sources look as follows: (1) GCR minimal average dose rate value is about $1 \mu\text{Gy h}^{-1}$ at $L=1$. It rises up to $10\text{-}11 \mu\text{Gy h}^{-1}$ at $L=4$ and stays further at this value up to $L=6.14$; (2) IRB (SAA) dose rates are about $22 \mu\text{Gy h}^{-1}$ at $L=1.1$. They rise sharply to a value of $600 \mu\text{Gy h}^{-1}$ at $L=1.4$ and then slowly decrease to a value of $20 \mu\text{Gy h}^{-1}$ at $L=2.8$; (3) ORB dose rates are at a value of $18 \mu\text{Gy h}^{-1}$ at $L=3.15$, rise up to a value of $500 \mu\text{Gy h}^{-1}$ at $L=4$ and then decrease down to a value of $80 \mu\text{Gy h}^{-1}$ at $L=6.14$.

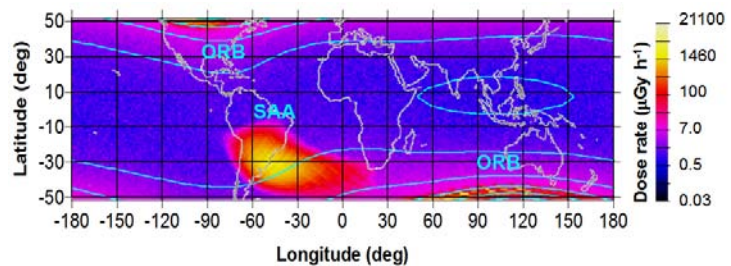


Figure 3. 3D geographic distribution of the dose rate data. The white (white blue) curves represent equal L-parameter values. South and north ORB regions are situated at $4.5 < L < 3.5$.

4. Comparison of R3DR data with model and other data

4.1. Comparison with Earth radiation models

In order to answer the question about the R3DR flux data representativeness, we prepared Fig. 4, which compares the fluxes measured by the R3DR instrument with those predicted by SPENVIS models: AE-8 MIN model (<http://www.spenvis.oma.be/>); Vette, 1991), CRRES/ELE model (<http://www.spenvis.oma.be/>); Meffert and Gussenhoven, 1994; Brautigam and Bell, 1995) and ESA-SEE1 model (<http://www.spenvis.oma.be/>); Vampola, 1996). The model conditions are as follows: Alt.=359 km; Lat.=48°S; UT=00:00; 0<Long.<180°; Step=2°; Low solar activity; Ap<15; Internal magnetic field model: (Jensen & Cain 1962) updated to 1996.8.

Figure 4 presents the flux longitudinal profile in the range 0°-180° as predicted by the models and measured by R3DR in the Southern Hemisphere at the conditions mentioned above. The Y axis presents the integral flux data in 5 orders of magnitude. All models and R3DR data have the same ($\text{cm}^{-2} \text{s}^{-1}$) dimension. The R3DR flux data (black points) are selected using the following criteria: 47°S<Lat.<49°S and dose rate higher than 100 $\mu\text{Gy h}^{-1}$. Analyzing flux and dose rate data in these latitudes we found that the area of extreme flux values is shifted by 10° to the east. The moving average line (dashed line) was found with a period of 100 points. It is seen that the R3DR data are at very low levels up to 55°E. We explain the subsequent maxima formed in the range 70°E-160°E with a concentration of descending orbits paths of the station. The R3DR data distribution is almost random in the whole range of longitudes 50°E-170°E with some tendency of maximum at 70°E-80°E. The shape of the R3DR data is closer to the CRESS model, which has a maximum in 110°E-120°E and this maximum coincides with L value maximum for this profile.

The other 2 models AE-8 MIN and ESA-SEE1, (ESA-SEE1 is an update of the AE-8 MIN model, Vampola, 1996) show a very similar longitudinal distribution with a maximum at 60°E-70°E. The common feature of the 3 models is that the predicted fluxes are orders of magnitudes higher than the experimental data. This large difference can be explained in two possible ways. The first one is the uncertainties of the models, which is manifested by the different shapes and place of extreme values calculated by the three models. The second one is connected with the loss of counts in the R3DR spectrometer.

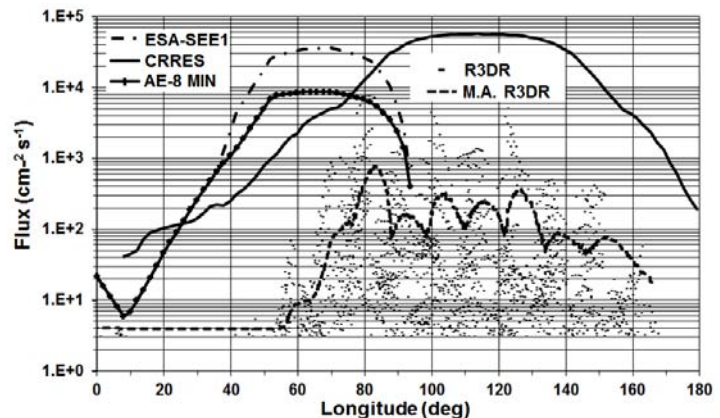


Fig. 4. Comparison of the R3DR data with the AE-8 MIN, ESA-SEE1 and CRRES/ELE models on the longitudinal profile at 48°S latitude.

For the 10 s time resolution spectra of R3DR we never observed overflow of the counts in one channel above the maximum allowed count limit of 65,536 counts per channel; that is why we consider that the dead time of the spectrometer can be the main reason for count losses. By analyzing RADOM instrument flux data inside the maximum of outer radiation belt we found that Liulin type instruments do have a real upper limit of flux values of 20,000 $\text{cm}^{-2} \text{s}^{-1}$ (Dachev et al., 2011). In fact in the R3DR data, the flux values are less than 10,000 $\text{cm}^{-2} \text{s}^{-1}$, which means that most of the differences between R3DR flux data and models are because of the uncertainties of the models.

4.2. Comparison with other measurements

Figure 5 presents the results of the comparison between R3DR data and the Japanese GOSAT data for the differential flux of electrons with energies between 0.91 and 1.06 MeV. Both data sets are ordered in the same way in two panels where the bottom panel is for the R3DR data, while the top is for the GOSAT data. GOSAT data are obtained graphically from the presentation "Space Environment Measurements by JAXA Satellites and ISS" of T. Obara at 7th European Space Weather Week, 15-19 November, 2010 - Brugge, Belgium, 2010 (Obara, 2010). On the X axis the UT is plotted for the period 01/04/-07/05/2011. On the Y axis the L value of the R3DR data in the range 2.5-6.5 is plotted. The GOSAT data are distributed up to L=9 but here only part of these data are presented.

The 3rd dimension of both panels is as follows: Figure 5a contains the GOSAT differential electron flux data with energies logarithmically coded between 0.91 and 1.06 MeV. Data are with dimension $\text{cm}^{-2} \text{s}^{-1} \text{sr}^{-1} \text{MeV}^{-1}$; in Figure 10b the R3DR dose rate data are plotted. At first glance both dimensions are not comparable but looking again at Figure 5 we see that there is a linear dependence between the dose rate and flux for the relativistic electrons finger. From this data

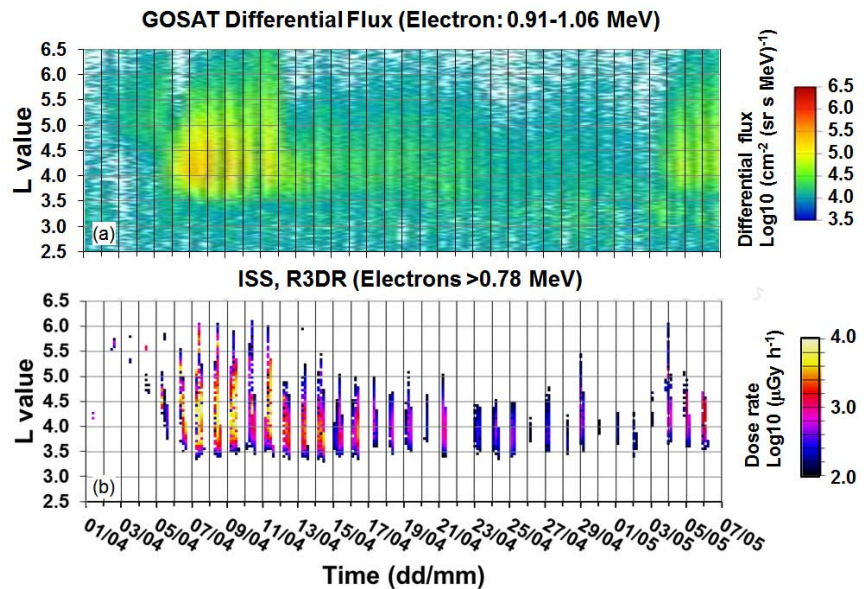


Fig. 5. Comparison of the R3DR dose rate data with the GOSAT 0.91-1.06 MeV relativistic electrons data for the period 01/04/-07/05/2010.

equation we obtain: $(\text{Dose rate})=2.34*\text{Flux}+15$, which means that the R3DR flux data are by a factor of 2.34 less than the dose rate values shown. The main conclusion for the absolute values is that the GOSAT fluxes are on the order of hundreds of thousands of particles per square cm per s, while the R3DR data show about 2 orders of magnitudes less. This is understandable because the GOSAT orbit is 300 km higher than the ISS orbit.

On the other hand, the purpose of Fig. 5 is mainly to compare the boundaries of the REP in L-value and the time and place of the extreme values obtained for both satellites. By analysing these parameters, we may conclude the following: (1) both data sets show similar lowering of the equatorward L value boundary of the precipitation from about $L=5$ on 1st of April down to $L=3.5$ on 6th of April. Later on this boundary stays stable around the value of 3.5 during the whole period; (2) the poleward boundaries of the precipitations also coincide quite well for the beginning of the period, reaching $L=6.5$ in the period 7-11 April and falling down later. The poleward boundaries of R3DR data on 5th and 6th of May are lower than the boundaries; (3) the temporal poleward movement of the precipitation boundary on 13th of April is well seen in both data, but later, on 21st and on 29th of April the GOSAT movement of the precipitation boundary is missing; (4) Both data show the absolute maximum of the precipitation of relativistic electrons on 7th of April.

Using the opportunity provided by (Zapp, 2011) and by 'Coordinated Data Analysis Web' at Goddard Space Flight Center (<http://cdaweb.gsfc.nasa.gov/>), we compare ISS TEPC data on 7th of April 2010 with the R3DR data and find that even inside ISS the TEPC record some additional relativistic electrons dose rate in the Southern Hemisphere crossings of the high latitude region. The highest caused by relativistic electrons and bremsstrahlung TEPC absorbed dose rate occur exactly when the R3DE reached it absolute maximum at almost $19000 \mu\text{Gy h}^{-1}$ at about 13:20 UT on 7th of April. The TEPC dose rate rises only from the GCR level of about 16 up to $40 \mu\text{Gy h}^{-1}$.

Also using information from (Obara, 2010) we looked at the global maps obtained by the Japanize instrument SDOM at ISS http://seesproxy.tksk.jaxa.jp/fw_e/dfw/SEES/pub/SEDA-AP/GRAPH and found that the ISS 0.93-1.85 MeV electron flux is enhanced in both Hemispheres equatorward from the magnetic poles in the period 7-9 April 2010. This is in accordance with the R3DR observations shown on the global distribution in Fig. 3.

Conclusions

Measurements of relativistic electrons were performed with 10 s resolution with the R3DR instrument outside the Russian Zvezda module of the ISS for the period March 2009-August 2010. The calculated stopping energy of normally incident particles to the detector is 0.78 MeV for electrons and 15.8 MeV for protons. The observations were correlated with the GOES-11 more than 2 MeV daily fluences and with daily Ap indexes. The selection of the data was done using the existing Liulin type instruments dose to flux relations, which define that when the dose to flux ratio in one exposition cycle is less than $1 \text{ nGy cm}^{-2} \text{ part}^{-1}$ the predominant amount of particles are electrons and vice versa, when this ratio is larger than 1, the predominant particles are protons. REP is seen in both Hemispheres above 45°N and 42°S geographic latitudes. The Northern Hemisphere REP dose rate values are

situated in a single area between 50°W and 130°W with a maximum at 90°W. In the Southern Hemisphere the REP is a wide area between 20°E and 170°W. A well-defined maximum is formed at about 70-80°E. The REP regions are seen in both Hemispheres as bands of high dose rate values in the range $3.5 < L < 4.5$. Maximal dose rate from the precipitating high energy electrons was found on 6th of April with highest dose rates of almost $22,000 \mu\text{Gy h}^{-1}$. The highest daily dose rate was reached on 7th of April with $2323 \mu\text{Gy day}^{-1}$. The comparison of the R3DR longitudinal flux profile along 48°S latitude with the AE-8 MIN, ESA-SEE1 and CRRES/ELE models shows that the three models predicted fluxes, which are orders of magnitudes higher than the experimental data. We attribute these large differences to the models uncertainties because we never observe overflow of the counts limits in one channel and because the flux is less than the real upper limit of Liulin instruments flux value of $20,000 \text{ cm}^{-2} \text{ s}^{-1}$. The comparison between R3DR data and Japanize GOSAT data shows good agreements for the places and dynamics of the REP boundaries obtained at both spacecraft.

Acknowledgements

This work was supported by the Bulgarian Academy of Sciences and partially by grant DID 02/08 of the Bulgarian Science Fund.

References:

1. Badhwar, G.D., Konradi, A., Braby, L.A., Atwell, W., Cucinotta, F.A., Measurements of trapped protons and cosmic rays from recent shuttle flights, *Adv. Space Res.*, 14, 67–72, 1994.
2. Brautigam, D.H. and Bell, J.T. CRRESELE documentation, PL-TR-95-2128. Environmental Research Papers, 1178, Phillips Laboratory, 1995.
3. Brown, J.C., and Stone, E.C. High-energy electron spikes at high latitudes. *J. Geophys. Res.* 77, 3384-3391, 1972.
4. Dachev, T., Atwell, W., Semones, E.; Tomov, B., Reddell, B. ISS Observations of SAA radiation distribution by Liulin-E094 instrument. *Adv. Space Res.* 37, 1672-1677, 2006.
5. Dachev, Ts. P., B. T. Tomov, Yu.N. Matviichuk, P.I. G. Dimitrov, Vadawale, S. V., J. N. Goswami, V. Girish, G. de Angelis, An overview of RADOM results for Earth and Moon Radiation Environment on Chandrayan-1 Satellite, *Adv. Space Res.*, 48, 5, 779-791, 2011. doi: 10.1016/j.asr.2011.05.009
6. Dachev, Ts.P., B.T. Tomov, Yu.N. Matviichuk, P.G. Dimitrov, N.G. Bankov, Relativistic Electrons High Doses at International Space Station and Foton M2/M3 Satellites, *Adv. Space Res.*, 1433-1440, 2009. doi:10.1016/j.asr.2009.09.023
7. Dachev, Ts. P., Characterization of near Earth radiation environment by Liulin type instruments, *Adv. Space Res.*, 1441-1449, 2009. doi:10.1016/j.asr.2009.08.007
8. Fürst, F., J. Wilms, R.E. Rothschild, K. Pottschmidt, D.M. Smith, R. Lingenfelter, Temporal variations of strength and location of the South Atlantic Anomaly as measured by RXTE, *Earth and Planetary Science Letters*, 281, 125–133, 2009.
9. Green, J.C, W.F. Denig, J.V. Rodriguez, H.J. Singer, T.M. Lotoaniu and D. Biesecker, D.C. Wilkinson, Space Weather Conditions at the Time of the Galaxy 15 Spacecraft Anomaly, 7th European Space Weather Week, 15-19 November, 2010 - Brugge, Belgium, 2010. <http://www.sidc.be/esww7/presentations/2.8.ppt>
10. Heynderickx, D., J. Lemaire, and E. J. Daly, Historical Review of the Different Procedures Used to Compute the L-Parameter, *Radiat. Meas.*, 26, 325-331, 1996.
11. Horneck, G., D.D. Win-Williams, R.L. Mancinelli, J. Cadet, N. Munakata, G. Ronto, H.G.M. Edwards, B. Hock, H. Waenke, G. Reitz, T. Dachev, D.P. Haeder, and C. Briollet, Biological experiments on the EXPOSE facility of the International Space Station, Proceedings of the 2nd European Symposium - Utilisation of the International Space Station, ESTEC, Noordwijk, 16-18 November 1998, SP-433, pp. 459-468, 1998.
12. Imhof, W. L., H. D. Voss, D. W. Datlowe, E. E. Gaines, J. Mobilia, and D. S. Evans, Relativistic electron and energetic ion precipitation spikes near the plasmopause, *J. Geophys. Res.*, 91, 3077-3088, 1986.
13. Imhof, W. L., H. D. Voss, J. Mobilia, D. W. Datlowe, and E. E. Gaines, The precipitation of relativistic electrons near the trapping boundary. *J. Geophys. Res.*, 96, 5619-5629, 1991.
14. Jensen, D. C., and J. C. Cain, An Interim Geomagnetic Field, *J. Geophys. Res.*, 67, 3568, 1962.
15. McIlwain, C. E., Coordinates for Mapping the Distribution of Magnetically Trapped Particles, *J. Geophys. Res.*, 66, pp. 3681-3691, 1961.
16. Meffert, J.D., and M.S. Gussenhoven, CRRES/PRO Documentation, PL-TR-94-2218, Environmental Research Papers, 1158, Phillips Laboratory, 1994.

17. Nealy, J. E., F. A. Cucinotta, J. W. Wilson, F. F. Badavi, N. Zapp, T. Dachev, B.T. Tomov, E. Semones, S. A. Walker, G. de Angelis, S. R. Blattnig, W. Atwell, Pre-engineering spaceflight validation of environmental models and the 2005 HZETRN simulation code, *Adv. Space Res.*, 40, 11, 1593-1610, 2007. doi:10.1016/j.asr.2006.12.030
18. Obara, T., Space Environment Measurements by JAXA Satellites and ISS, 7th European Space Weather Week, 15-19 November, 2010 - Brugge, Belgium, 2010. <http://www.sidc.be/esww7/presentations/2.5.ppt>
19. Reitz, G., R. Beaujean, E. Benton, S. Burmeister, T. Dachev, S. Deme, M. Luszik-Bhadra, P. Olko, Space radiation measurements on-board ISS-The DOSMAP experiment, *Radiat. Prot. Dosim.* 116 (1-4), 374-379, 2005.
20. Slaba, T.C., S.R. Blattnig, F.F. Badavi, N.N. Stoffle, R.D. Rutledge, K.T. Lee, E.N. Zappe, T.P. Dachev and B.T. Tomov, Statistical Validation of HZETRN as a Function of Vertical Cutoff Rigidity using ISS Measurements, *Adv. Space Res.*, 47, 600-610, 2011. doi:10.1016/j.asr.2010.10.021
21. Vampola, A. L., Outer Zone Energetic Electron Environment Update, Final Report of ESA/ESTEC, 1996.
22. Vette, J.I., The NASA/National Space Science Data Center Trapped Radiation Environment Model Program (1964-1991), NSSDC/WDC-A-R&S 91-29, 1991.
23. Wilson, J.W., Nealy, J.E., Dachev, T.P., Tomov, B.T., Cucinotta, F. A., Badavi, F. F., DeAngelis, G., Leutke, N., Atwell, W. Time serial analysis of the induced LEO environment within the ISS 6A, *Adv. Space Res.*, 40, 1562-1570, 2007. . doi:10.1016/j.asr.2006.12.030
24. Wrenn G.L., Chronology of 'killer' electrons: Solarcycles 22 and 23, *J. Atmos. Solar-Terr. Phys.*, 71, 1210-1218, 2009.
25. Zapp, N., NASA GSFC, by 'Coordinated Data Analysis Web' at Goddard Space Flight Center, <http://cdaweb.gsfc.nasa.gov/tmp/>, May, 2011.
26. Zheng, Y., Lui, A.T.Y., Li, X. and Fok, M. - C., Characteristics of 2-6 MeV electrons in the slot region and inner radiation belt, *J. Geophys. Res.*, 111, A10204, 2006. doi:10.1029/2006JA011748